Simulations of Ripple Formation on Ion-Bombarded Solid Surfaces

I. Koponen,* M. Hautala,† and O.-P. Sievänen
Department of Physics, University of Helsinki, P.O. Box 9, FIN-00014 Helsinki, Finland
(Received 7 October 1996)

Ripple formation on amorphous carbon surfaces bombarded by 5 keV Ar ions is studied by atomistic simulations. Sputtering is treated in detail by simulating the entire collision cascades originated by the bombarding Ar ions. Surface relaxation is described by a Wolf-Villain-type discrete model. Ripples and wavelike patterns are observed to emerge on the surface. The ripples have a well-defined wavelength and the orientation of the wave crests changes from normal to parallel to the beam, when the angle of incidence is increased from 30° to 60°, respectively. The wavelength is found to depend on the magnitude of the diffusion and orientation of the beam as predicted by the continuum theories. [S0031-9007(97)02870-6]

PACS numbers: 79.20.Rf, 64.60.Ht, 68.35.Bs

Ion bombardment of solid surfaces is known to create curious morphologies ranging from self-affine surface roughness [1] to "fingerprint"-like structures and even regular waves or ripples [2,3]. The formation of ripples occurs usually on a length scale of micrometers, but in some cases ripples are observed also on the submicrometer scale [4]. The formation of ripples can be understood in terms of the linear instability caused by surface curvature dependent sputtering [5–7]. The instability, described as a "negative surface tension," competes with surface diffusion and this interplay generates ripples with wavelength $\lambda \propto \sqrt{K/|\nu|}$, where K is the surface diffusivity and ν the negative surface tension [5–7]. Ripples may occur either in the direction parallel or normal to the bombarding beam, depending on the anisotropy due to oblique incidence of the ion beam [5–7].

The interest towards ripple formation has recently been renewed by the notion that it belongs to the class of dynamical systems described by the Kuramoto-Sivashinsky (KS) equation and its noisy generalizations [6,7]. The current continuum models give a rather complete picture of the ripple formation on the micrometer scale where $\lambda \approx 1\ \mu$m and when local slopes of the surface are moderate. The derivation of the continuum equations from the underlying more detailed rate equation describing the sputtering erosion has been accomplished only quite recently [8]. By connecting continuum models with microscopic dynamics it becomes possible to study the role the fluctuations of the sputtering processes have in the formation of ripples.

In order to make further and complementary progress in bridging the continuum models and realistic microscopic dynamics we have conducted for the first time simulations of ripple formation, which are microscopic and realistic in the sense that erosion of the surface occurs by a sputtering of single atoms emerging from collision cascades calculated in detail, collision by collision, using a Monte Carlo method. We used recently a similar approach to study the self-affine roughness on the submicrometer scale [9]. We are interested of the submicrometer-scale behavior, and thus simulations can be performed with moderate or suppressed diffusion. This restriction is essential also for the feasibility of atomistic simulations in the level of realism of the present study.

The simulations were carried out using a modified version of the computer code COSIPO [9,10], initially devised to simulate the implantation of energetic heavy ions in solid targets. This code is known to correctly describe (for comparison with other similar codes, see Ref. [11]) most kinetic impact phenomena such as sputtering [10]. The collision cascades are simulated in the so called binary collision approximation. The interaction between atoms is described by a screened Coulomb potential, which gives accurate collision cross sections and sputtering yields at the energies involved in the present study [10]. Erosion of surface occurs as an ejection of single atoms, which are moving outwards from the (local) surface with the kinetic energy exceeding the surface binding energy $E_b = 7.5$ eV, derived from the heat of sublimation [9]. The surface area is limited to 500×75 atoms (about 100×15 nm^2) and the target is divided into boxes, which contain a single carbon atom. For sputtering, the position of atoms is treated as a continuous variable, but for diffusion the underlying lattice structure is used. The other modifications of the code, which make it possible to rapidly update the surface structure, are as explained in our previous works [9,10]. Every sputtering process is simulated in detail and takes into account the instantaneous local surface topography, and then all shadowing effects and local fluence variations due to surface curvature are correctly described in the simulations.

The surface diffusion is described by using a simplified model of irreversible relaxation, containing, however, the essential physics of the surface diffusion [9]. The model closely resembles the Wolf-Villain [12] and Tamborenea–Das Sarma [13] models and it is based on the irreversible jumps of atoms guided by the rule to maximize the bonding or the number of the nearest neighbors. The available

 0031-9007/97/78(13)/2612(4)$10.00

sites are either within the distance of nearest neighbors (relaxation model R1) or next nearest neighbors (model R2). The relaxation process for all surface atoms in the sample is realized after the completion of collision cascade originated by each impinging ion (for more details, see Ref. [9]). Each atom completes the diffusion process instantaneously and then there are no problems with transient effects due to competing kinetic rates and continuous migration of atoms [12,13].

Simulations were performed for amorphous carbon surfaces bombarded by 5 keV Ar ions. Examples of the topography of the surface (relaxation described by model R2) bombarded at oblique incidence at angles $\Theta = 30°$ and $\Theta = 60°$ (relative to the surface normal) are shown in Fig. 1. At both angles of incidence the ripples are clearly seen. The slopes of the ripples are 7°–14°, larger than the slopes 2°–5° found in experiments [2], where diffusion is always larger than in cases studied here. For the angle $\Theta = 30°$ the ripple wave vector is parallel (wave crests are perpendicular) to the beam, and when the incidence angle is increased to $\Theta = 60°$, a regular wave pattern with the wave vector normal (crests parallel) to the beam direction emerges. This rotation of the wave crests is in complete agreement with theoretical predictions based on the continuum models [5–7].

In both cases shown in Fig. 1 the calculational cell was approximately 100 nm × 15 nm, the larger side oriented in the direction of the wave vector of the ripples. In order to be convinced that the results are not artifacts of the simulation method or the boundary conditions, various cell sizes and forms were tested, in particular, the computational cells were rotated. The ripple pattern is always easily detected and the wavelength remains unaffected, although for too small cells the ripples are more irregular than those shown in Fig. 1.

The traveling of ripples, predicted by the linear theory [5–7], is also seen in the simulations. This phenomenon is clearly visible in Fig. 2, where a gray-level plot of surface topography corresponding to model R2 is shown at various stages of bombardment. The traveling is caused by the sputtering induced drift and it can be related to the derivative of the sputtering yield with respect to the angle of incidence [5].

The wavelength of the ripples is obtained from the height-height correlation function $G(\mathbf{r}) \propto \sum_{\mathbf{k}} \exp[-i\mathbf{k} \cdot \mathbf{r}]S(\mathbf{k})$, where $S(\mathbf{k}) = \langle \hat{h}(-\mathbf{k})\hat{h}(\mathbf{k})\rangle$ is the structure factor calculated from the Fourier transform $\hat{h}(\mathbf{k})$ of instantaneous surface positions. The correlation function $G(\mathbf{r})$ is shown for the pertinent direction x or y (the other direction is averaged out) in Fig. 3 at various stages in the course of bombardment. The peaks with approximately integer multiplicity of the first peak are clearly visible, allowing the determination of the wavelength of the ripples. For comparison, peak positions based directly on the structure factor $S(\mathbf{k})$ are denoted by arrows. Note that clear signs of the ripples begin to emerge only after a bombardment with relatively high fluences. The wavelength of the ripples for the incidence angle $\Theta = 60°$ is $\lambda_{R2}(60°) \approx (19 \pm 1)$ nm, which is approximately 1.4 times the wavelength $\lambda_{R2}(30°) \approx (14 \pm 1)$ nm obtained at an angle $\Theta = 30°$. Calculating the negative surface tensions ν_x and ν_y based on the linear theory [5,6], we obtain at the present case $\lambda(60°)/\lambda(30°) \propto$

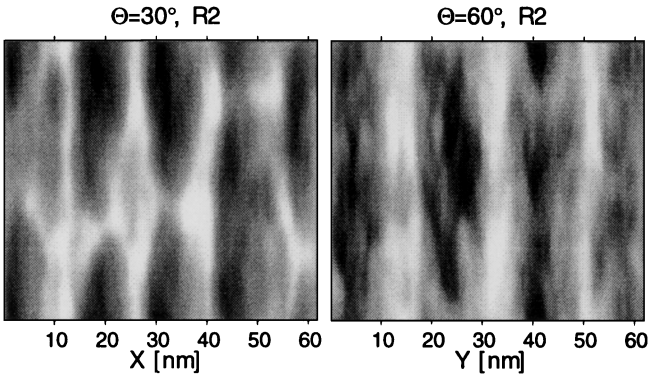

FIG. 1. Ripple formation on carbon surface due to 5 keV Ar ion bombardment at an angle of incidence $\Theta = 30°$ and 60° (relative to surface normal). Surface relaxation is described by model R2 in both cases. The bombarding beam is in the direction of the x axis in the (x, z) plane. The cases shown are for fluences 3.1×10^{17} ions/cm^2 and 1.3×10^{17} ions/cm^2 for $\Theta = 30°$ and $\Theta = 60°$, respectively. In both cases the mean surface recession is of similar magnitude. The shown area is 60×15 nm^2 of the total cell 100×15 nm^2. Note that in the direction of the crests (i.e., the vertical direction) the scale is expanded for better visibility. In the gray-level plots the dark regions are below and the light regions above the mean position of the surface.

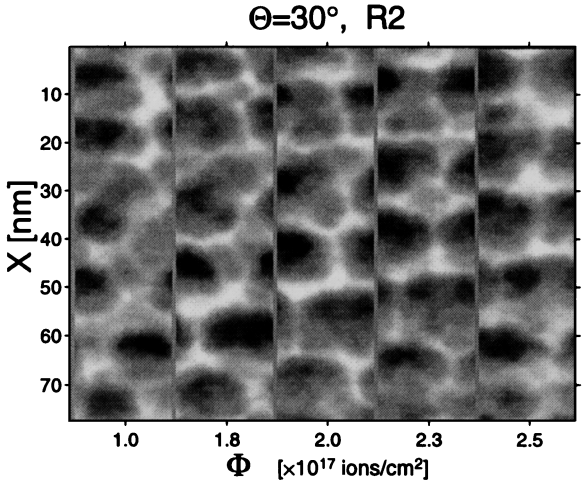

FIG. 2. Traveling of ripples. The surface structure resulting from the bombardment at an angle $\Theta = 30°$ is shown at different stages of bombardment. The area shown is 60×15 nm^2 of the total cell 100×15 nm^2 in all cases. The bombarding beam is now in the vertical direction (relative to the figures shown) and it hits the crests from the bottom edge of the cells.

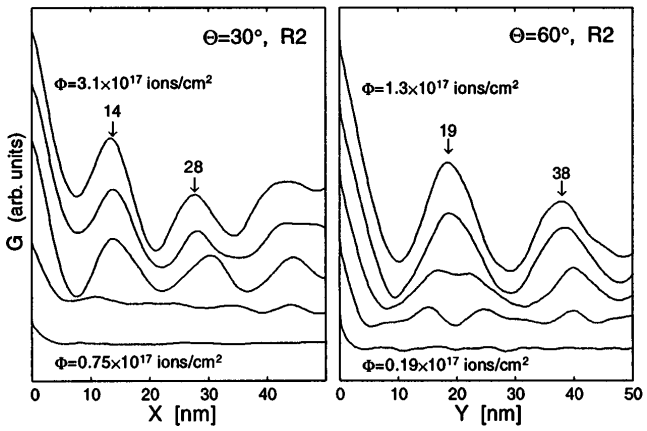

FIG. 3. Height-height correlation functions $G(r)$ at the pertinent direction (the other direction is averaged out) corresponding to situation shown in Fig. 1. Positions shown by arrows are inferred from the structure factor. Smallest and largest fluences are denoted, and some intermediate cases at approximately equidistant intervals are shown.

$\sqrt{\nu_x(30°)/\nu_y(60°)} \approx 1.7$, which is not far from the value found in the simulations.

The effect of diffusion is seen by comparing the calculations with relaxation model R2 to results based on model R1 and to calculations without relaxation (model R0). The gray-level plots of the surface topography in the case of models R1 and R0 are shown in Fig. 4. The height-height correlation functions $G(\mathbf{r})$ for the different models are summarized in Fig. 5, where also the peak positions inferred directly from the structure factor are shown. Comparing the wavelengths it is seen that they are larger for faster diffusion (longer jump lengths), which is in qualitative agreement with the theoretical scaling. For the diffusion model used here, there is no direct relationship between the diffusion coefficient K and relaxation length l, and therefore more quantitative comparison is beyond the scope of the model.

In the case of no diffusion, in the angle of incidence $\Theta = 60°$ regular ripples are still seen with wavelength approximately twice the rms spread of the cascade. The ripples for $\Theta = 30°$ are more distorted and they nearly disappear in the absence of the diffusion. Regular ripples appear only at low fluences, and the ripple patterns are destroyed or severely distorted when bombardment is continued. The strong distortion of the ripple patterns is reminiscent of the behavior found in Ref. [7] at the onset of nonlinearities in the KS equation. Although formation of patterns (at least mounds) on the scale of the cascade can be expected in the absence of surface diffusion, the appearance of ripples is more puzzling. However, it has been recently shown that surface topography dependent sputtering can induce an additional relaxation mechanism which can be described as an ion-induced diffusion [14]. In the simulations, where surface height variations are treated without approximations, this effect should also be present, which explains the appearance of the ripples without relaxation.

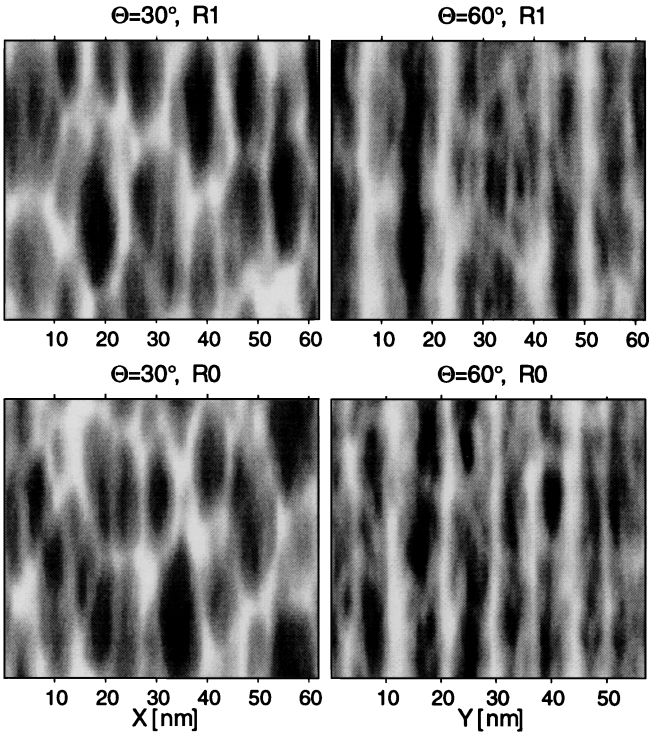

FIG. 4. The effect of diffusion on the ripple formation. The angle of incidence and the model of surface relaxation are denoted. The fluences corresponding to the situation shown are for model R1 approximately 2×10^{17} ions/cm^2 and for model R0 5×10^{16} ions/cm^2. Otherwise similar to Fig. 1.

The results presented here demonstrate the feasibility of detailed atomistic simulations in the description of the ripple formation in surface erosion. Because of restrictions on the reasonable computing times we are restricted to cell sizes and magnitudes of diffusion treated here. There is no basic obstacle extending the simulations

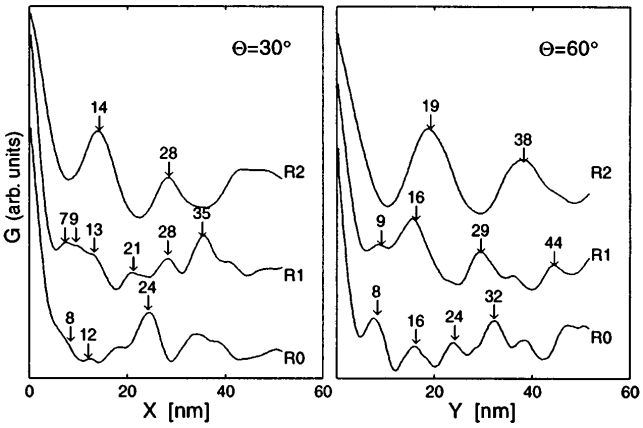

FIG. 5. Height-height correlation functions corresponding to the situations displayed in Figs. 1 and 3. Positions shown by arrows are inferred from the structure factor.

in the domain of more realistic diffusion, but the cost of the computations then increases rapidly. On the other hand, the simulations are most useful in the studies of submicrometer-scale phenomena, where steep local slopes bring in some new interesting features such as shadowing, twisting, and pinching off of the ripples. Shadowing is probably not a very important effect, but from the theoretical point of view it would be interesting to know how it affects the ripple formation, because shadowing is known to belong in a universality class of its own [15]. Another detail needing a closer study is the effect of the redeposition, but it warrants a separate study of its own.

In conclusion, we have reported the first atomistic and thus far most realistic simulations of the formation of ripples on the ion-bombarded solid surfaces. The ripple formation is studied in the presence of moderate or suppressed diffusion, when ripples occur on the submicrometer scale. Simulations show that the orientation of the ripples depend on the angle of incidence of the bombarding beam and travel as expected on the basis of the continuum theories. The dependence of the ripple wavelength on the magnitude of the surface diffusion and on the effective negative surface tension is also in qualitative agreement with theoretical scaling. The general features of the ripple formation revealed by the simulations thus support the recent theoretical views of the ripple formation.

*Corresponding author; electronic address: ismo.koponen@helsinki.fi

†Permanent address: Department of Agricultural and Household Technology, University of Helsinki, P.O. Box 27, FIN-00014 Helsinki, Finland.

[1] E. A. Eklund, R. Bruinsma, J. Rudnick, and R. S. Williams, Phys. Rev. Lett. **67**, 1759 (1991); J. Krim, I. Heyvaert, C. Van Haesendonck, and Y. Bruynseraede, Phys. Rev. Lett. **70**, 57 (1993).

[2] G. W. Lewis, M. J. Nobes, G. Carter, and J. L. Whitton, Nucl. Instrum. Methods **170**, 363 (1980); G. Carter, V. Vishnyakov, and M. J. Nobes, Nucl. Instrum. Methods Phys. Res., Sect. B **115**, 440 (1996).

[3] E. Chason, T. M. Mayer, B. K. Kellerman, D. T. McIlroy, and A. J. Howard, Phys. Rev. Lett. **72**, 3040 (1994); T. M. Mayer, E. Chason, and A. J. Howard, J. Appl. Phys. **76**, 1633 (1994); E. Chason, T. M. Mayer, and A. J. Howard, Mater. Res. Soc. Symp. Proc. **317**, 91 (1994).

[4] S. I. Park, A. Marshall, R. H. Hammond, T. H. Geballe, and J. Talvechio, J. Mater. Res. **2**, 446 (1987).

[5] R. M. Bradley and J. M. E. Harper, J. Vac. Sci. Technol. A **6**, 2390 (1988).

[6] R. Cuerno and A.-L. Barabási, Phys. Rev. Lett. **74**, 4746 (1995); R. Cuerno and K. B. Lauritsen, Phys. Rev. E **52**, 4853 (1995).

[7] M. Rost and J. Krug, Phys. Rev. Lett. **75**, 3894 (1995).

[8] R. Cuerno, H. A. Makse, S. Tomassone, S. T. Harrington, and H. E. Stanley, Phys. Rev. Lett. **75**, 4464 (1995); K. B. Lauritsen, R. Cuerno, and H. A. Makse, Phys. Rev. E **54**, 3577 (1996).

[9] I. Koponen, M. Hautala, and O.-P. Sievänen, Phys. Rev. B **54**, 13 502 (1996); M. Hautala and I. Koponen, Nucl. Instrum. Methods Phys. Res. Sect. B **117**, 95 (1996).

[10] M. Hautala, Phys. Rev. B **30**, 5010 (1984); M. Hautala and J. Likonen, Phys. Rev. B **41**, 1759 (1990).

[11] K. Gärtner *et al.,* Nucl. Instrum. Methods Phys. Res., Sect. B **102**, 183 (1995).

[12] D. E. Wolf and J. Villain, Europhys. Lett. **13**, 389 (1990); P. Šmilauer and M. Kotrla, Phys. Rev. B **49**, 5769 (1994).

[13] S. Das Sarma and P. Tamborenea, Phys. Rev. Lett. **66**, 325 (1991); S. Das Sarma and S. V. Ghaisas, Phys. Rev. Lett. **69**, 3762 (1992).

[14] M. A. Makeev and A.-L. Barabási, Report No. cond-mat/9701116.

[15] J. Krug and P. Meakin, Phys. Rev. E **47**, R17 (1993).